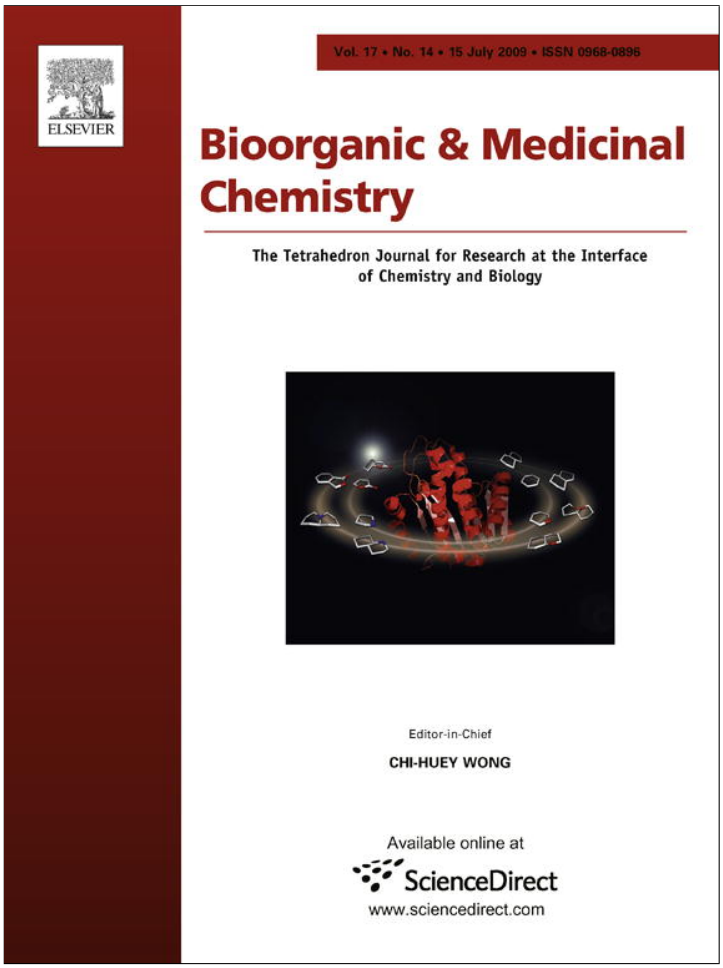

Bioorganic & Medicinal Chemistry 17 (2009) 5146–5152

Contents lists available at ScienceDirect

Bioorganic & Medicinal Chemistry

journal homepage: www.elsevier.com/locate/bmc

Inhibition of human vascular NADPH oxidase by apocynin derived oligophenols

Mauricio Mora-Pale [a], Michel Weïwer [b], Jingjing Yu [c], Robert J. Linhardt [a,b,c,*], Jonathan S. Dordick [a,c,*]

[a] Department of Chemical and Biological Engineering, Center for Biotechnology and Interdisciplinary Studies, Rensselaer Polytechnic Institute, Troy, NY 12180, USA
[b] Department of Chemistry and Chemical Biology, Center for Biotechnology and Interdisciplinary Studies, Rensselaer Polytechnic Institute, Troy, NY 12180, USA
[c] Department of Biology, Center for Biotechnology and Interdisciplinary Studies, Rensselaer Polytechnic Institute, Troy, NY 12180, USA

ARTICLE INFO

Article history:
Received 7 March 2009
Revised 19 May 2009
Accepted 22 May 2009
Available online 30 May 2009

Keywords:
Apocynin
Peroxidase catalysis
Inhibition of NADPH oxidase
Oligophenols

ABSTRACT

Enzymatic oxidation of apocynin, which may mimic in vivo metabolism, affords a large number of oligomers (apocynin oxidation products, AOP) that inhibit vascular NADPH oxidase. In vitro studies of NADPH oxidase activity were performed to identify active inhibitors, resulting in a trimer hydroxylated quinone (IIIHyQ) that inhibited NADPH oxidase with an IC_{50} = 31 nM. Apocynin itself possessed minimal inhibitory activity. NADPH oxidase is believed to be inhibited through prevention of the interaction between two NADPH oxidase subunits, $p47^{phox}$ and $p22^{phox}$. To that end, while apocynin was unable to block the interaction of his-tagged $p47^{phox}$ with a surface immobilized biotinylated $p22^{phox}$ peptide, the IIIHyQ product strongly interfered with this interaction (apparent IC_{50} = 1.6 μM). These results provide evidence that peroxidase-generated AOP, which consist of oligomeric phenols and quinones, inhibit critical interactions that are involved in the assembly and activation of human vascular NADPH oxidase.

1. Introduction

Recent years have seen substantial improvement in our understanding of the role of superoxide anion ($\cdot O_2^-$) in eliciting oxidative stress and vascular diseases.[1–5] The production of $\cdot O_2^-$ is catalyzed by a variety of enzymes, including xanthine oxidase, cytochromes P450, lipoxygenase, enzymes in the mitochondrial respiratory chain, and NADPH oxidases.[6] The latter, in particular, have been identified as the major source of $\cdot O_2^-$ in vascular endothelial cells (VECs). Excessive production of $\cdot O_2^-$ in VECs leads to increased oxidative stress and endothelial dysfunction. This in turn can result in a diverse array of cardiovascular diseases, including atherosclerosis, hypertension, diabetes, heart failure, stroke, and restenosis.[1,7–11]

The most well-studied NADPH oxidase in humans is found in neutrophils. In the resting state, the neutrophil enzyme consists of at least six partially dissociated components.[12] Tight regulation of NADPH oxidase activity is achieved by at least two mechanisms; the association of the cytosolic subunits and the modulation of reversible protein–protein and protein–membrane interactions.[13] Despite near 100% homology with the neutrophil NADPH oxidase,[14,15] the exact assembly and activation of VEC NADPH oxidase is poorly understood.[16] Nevertheless, current evidence suggests that phosphorylation of key serine residues in $p47^{phox}$ facilitates interaction of a Src homology 3 (SH3) domain of this protein with a proline-rich region (PRR) of $p22^{phox}$, thereby forming the active membrane-associated NADPH oxidase complex[17,18] (Scheme 1).

The catalytic subunit of NADPH oxidase (Nox) has several isoforms and, at least three of them are expressed in VEC (Nox1, Nox2, and Nox4). Their precise activation mechanisms and cellular regulation remain unclear.[19,20] Nox1 appears to be of only minor importance in the generation of VEC reactive oxygen species (ROS). Nox4, however, is abundantly expressed in endothelial cells, more than Nox2.[21] Nevertheless, Li et. al.[21] showed that, despite low expression relative to Nox4, under starvation conditions Nox2 was upregulated ~8-fold and, as a consequence of this nutrient deprivation-induced oxidative stress, the production of $\cdot O_2^-$ increased ~2.3-fold. Importantly, Nox2 requires assembly of $p47^{phox}$ with other cytosolic subunits prior to translocation to the membrane to form the active NADPH oxidase complex.[22,23]

Due to the key role VEC NADPH oxidase appears to play in vascular diseases, identification of selective inhibitors is of great interest. Along these lines, several inhibitors have been identified, including nitrovasodilators,[24] the flavonoid derivative 6,8-diallyl-5,7-dihydroxy-2-(2-allyl-3-hydroxy-4-methoxyphenyl)-1-*H*-benzo-[*b*]-pyran-4-one,[25] and peptides such as the antibiotic PR-39.[26] Interestingly, PRR regions are also known to bind polyphenols (such as flavonoids).[27] It is not surprising, therefore, that phenolics have been found to have NADPH oxidase inhibitory activity.

Apocynin (4′-hydroxy-3′-methoxyacetophenone)[28,29] is a particularly interesting phenol that has been used as inhibitor of NADPH oxidase. While apocynin itself was found to have low activity in vitro[29,30] metabolism in vivo converts the phenol into active metabolites that inhibit the enzyme.[30–34] This may be due to per-

* Corresponding authors. Tel.: +1 518 276 2899; fax: +1 518 276 2207 (J.S.D.).
E-mail addresses: linhar@rpi.edu (R.J. Linhardt), dordick@rpi.edu (J.S. Dordick).

0968-0896/$ - see front matter © 2009 Elsevier Ltd. All rights reserved.
doi:10.1016/j.bmc.2009.05.061

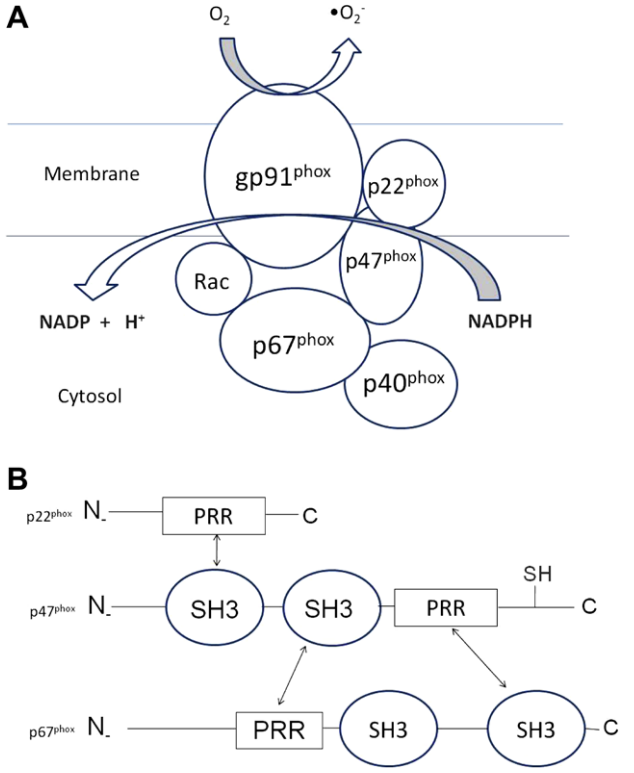

Scheme 1. (A) Active complex of NADPH oxidase. Cytosolic subunits (p47^{phox}, p67^{phox}, p40^{phox} and Rac 1 or 2 translocate to the membrane to bind p22^{phox} and catalytic gp91^{phox}. (B) Protein complexes (in the cytosol and membrane) occur by SH3 domain interactions with PRR.[7,13]

oxidase catalysis[29,30,35,36] leading to disruption of the p47^{phox}–p22^{phox} interaction, which is required for translocation of the cytosolic enzyme components to the membrane leading to activation of the enzyme complex. In the current work, we demonstrate that several oligomeric apocynin oxidation products generated by peroxidases are extremely potent inhibitors of VEC NADPH oxidase in vitro. Moreover, a strong correlation exists between the inhibition of VEC NADPH oxidase in endothelial cell-based assays and disruption of the interaction of EC p47^{phox}–p22^{phox} in cell-free assays. These results provide additional mechanistic insight into the nature and function of active metabolites of apocynin.

2. Results and discussion

Under conditions of oxidative stress, overactive NADPH oxidase in the vasculature generates $\cdot O_2^-$, thereby leading to increased levels of H_2O_2. In the presence of peroxidases in the blood, for example, myeloperoxidase, and reducing substrates of peroxidases, such as phenols, peroxidatic reactions can occur. To mimic this scenario, we used a simple commercially available peroxidase from soybean (SBP) to catalyze the oxidation of apocynin in the presence of H_2O_2 following our earlier published procedure.[37] Such reaction would then be expected to mimic peroxidatic metabolism in the vasculature.

Following the enzymatic oxidation of apocynin, a water-soluble fraction was extracted into ethyl acetate to give fraction AOP-1 and a chloroform soluble precipitate was fractionated by silica chromatography to yield nine fractions (AOP-2 to AOP-10). Each fraction was analyzed by LC–MS to qualitatively identify the AOP in each mixture, giving rise to the identification of oligomers in their demethylated, hydroxylated, or quinone forms (Table 1). The total conversion of the enzymatic reaction was ~50%; the precipitate representing 87% of the total products while 13% remained in the aqueous phase. The ability of each AOP fraction to inhibit VEC NADPH oxidase was then assessed at a dose range from 0 to 1000 μM (based on apocynin monomer unit mass), as determined by cytochrome *c* reduction for extracellular superoxide detection and by dihydroethidium (DHE) staining for intracellular superoxide detection.

2.1. NADPH oxidase activity—cytochrome *c* reduction

The NADPH oxidase inhibitory activity of apocynin and AOP fractions was assessed in an endothelial cell-based assay by measuring the generation of $\cdot O_2^-$ via cytochrome *c* reduction. Apocynin itself possesses minimal inhibitory activity (IC_{50} >1 mM; Fig. 1), which is consistent with reports in the literature.[29,30] However, the extracted water-soluble phase (AOP-1) exhibited an apparent IC_{50} value of 155 nM (Fig. 1), despite analysis of this mixture by NMR, TLC, and LC–MS, which indicated that the major component was unreacted apocynin (~90%). Thus, the inhibition of NADPH oxidase must result from the presence of at least one very strong NADPH oxidase inhibitor present in the remaining 10% of the water-soluble fraction. Following purification via silica chromatography, a trimer hydroxylated quinone (IIIHyQ, 508 *m*/*z*, Fig. 1) was identified as the major active compound in AOP-1, with strong inhibitory activity against VEC NADPH oxidase (IC_{50} = 31 nM).

A similar study was performed for the chloroform-soluble enzyme reaction precipitate, which following chromatographic separation, resulted in nine distinct fractions (AOP-2 through AOP-10, IC_{50} values summarized in Table 2). Fractions AOP-2–AOP-4 showed substantial NADPH oxidase inhibitory activity (<1.0 μM). Fractions AOP-1 and AOP-2 consisted of IIIHyQ along with other oligomeric species. AOP-4, however, consisted of other trimeric compounds, including trimeric quinones (IIIQ, IIIHy-MeQ, and III3-HyQ) that also inhibited NADPH oxidase. Higher oligomeric species (e.g., tetrameric to heptameric) showed relatively low inhibitory activity. These results demonstrate that some of the AOP possess strong VEC NADPH oxidase inhibitory activity, as reflected in the cell-based enzyme assay.

2.2. Intracellular superoxide detection—DHE staining

To establish the ability of AOP to suppress intracellular $\cdot O_2^-$ formation by NADPH oxidases, we used DHE staining of whole EC following incubation with apocynin, IIIHyQ, and phenylarsine oxide (PAO, an inhibitor of NADPH oxidase[39] and serving as a positive control). DHE is a cell-permeable reagent that reacts with $\cdot O_2^-$ to form oxyethidium,[38] which in turn interacts with nucleic acids to emit a bright red color detectable qualitatively by fluorescence microscopy. Figure 2 shows images of DHE stained EC after incubation with the aforementioned compounds. In the absence of compound, the EC fluoresce as a result of strong and expected $\cdot O_2^-$ production. Apocynin, even up to 1 mM, did not appreciably reduce this fluorescence (Fig. 2A). In contrast, IIIHyQ strongly reduced the $\cdot O_2^-$ induced fluorescence (Fig. 2B), which was consistent with the effect of the positive control compound (PAO, Fig. 2C). These results suggest that the IIIHyQ inhibits NADPH oxidase intracellularly. In addition, the inability of very high concentrations of apocynin to inhibit NADPH oxidase (as reflected in the lack of inhibition of $\cdot O_2^-$ production) also indicates that apocynin is unable to scavenge $\cdot O_2^-$.

2.3. Interaction between his-p47^{phox} protein and biotin-p22 peptide

The p47^{phox} and p22^{phox} protein subunits play a significant role in the activation of NADPH oxidase.[13] Translocation of p47^{phox}

Table 1
AOP present in soluble and precipitate fractions produced from the peroxidatic oxidation of apocynin based on LC–MS analysis. Nomenclature: A (apocynin), I (monomer), II (dimer), III (trimer), IV (tetramer), V (pentamer), VI (hexamer), VII (heptamer), Q (quinone), Hy (hydroxylated), -Me (demethylated)

Fraction	Components
AOP-1	A (166 *m*/*z*); II or IIHy-MeQ (330 *m*/*z*); IIIHyQ (508 *m*/*z*); III2Hy or III3HyQ (526 *m*/*z*); IV-3MeQ (614 *m*/*z*); IV or IVHy-MeQ (658 *m*/*z*)
AOP-2	A (166 *m*/*z*); III3OH (542 *m*/*z*); II or IIHy-MeQ (330 *m*/*z*); III4Hy-Me (530 *m*/*z*); IIIHyQ (508 *m*/*z*); III-Me (478 *m*/*z*); IIIHy (480 *m*/*z*); III-3Me (450 *m*/*z*); IV-Me (644 *m*/*z*), III-2MeQ (464 *m*/*z*), III-3Me (500 *m*/*z*), IV-Me (692 *m*/*z*)
AOP-3	II or IIHy-MeQ (330 *m*/*z*); III or IIIHy-MeQ (494 *m*/*z*); III-Me or IIIHy-2MeQ (480 *m*/*z*), IIIHyQ (508 *m*/*z*), IVHy (674 *m*/*z*); IV3Hy (706 *m*/*z*), IV3Hy-2Me (678 *m*/*z*), IV-2MeQ (628 *m*/*z*)
AOP-4	A (166 *m*/*z*); IIIHy (510 *m*/*z*); II or IIHy-MeQ (330 *m*/*z*); III3Hy (542 *m*/*z*); IVHy (674 *m*/*z*); III2Hy or III3HyQ (526 *m*/*z*); IIIQ (492 *m*/*z*); III or IIIHy-MeQ (494 *m*/*z*)
AOP-5	A (166 *m*/*z*); II or IIHy-MeQ (330 *m*/*z*); IV (658 *m*/*z*); III3Hy (542 *m*/*z*); III-2Me (466 *m*/*z*); III2Hy or III3HyQ (526 *m*/*z*); IV4Hy-3Me (680 *m*/*z*); III or IIIHy-MeQ (494 *m*/*z*); IV or IVHy-MeQ (658 *m*/*z*); IIIQ(492 *m*/*z*); III-3Me (500 *m*/*z*); VHy-MeQ (822 *m*/*z*)
AOP-6	II or IIHy-MeQ (330 *m*/*z*); III or IIIHy-MeQ (494 *m*/*z*); IV2Hy (690 *m*/*z*); III-3Me (452 *m*/*z*); IV4Hy-3Me (680 *m*/*z*); IV or IVHy-MeQ (658 *m*/*z*); IV-3Me (616 *m*/*z*), V4Hy-3Me (844 *m*/*z*); VII4Hy-2Me (1186 *m*/*z*) V or VHy-MeQ (822 *m*/*z*)
AOP-7	III3Hy (500 *m*/*z*); II or IIHy-MeQ (330 *m*/*z*); III or IIIHy-MeQ (494 *m*/*z*); VI5Hy-4Me (1010 *m*/*z*), IIQ (328 *m*/*z*); IV2Hy (690 *m*/*z*); IV4Hy-3Me (680 *m*/*z*); VI4Hy-3Me (1008 *m*/*z*); IV or IVHy-MeQ (658 *m*/*z*)
AOP-8	II or IIHy-MeQ (330 *m*/*z*); IV5Hy-4Me (682 *m*/*z*); III3Hy-2Me (514 *m*/*z*); IVHy (674 *m*/*z*); IV or IVHy-MeQ (658 *m*/*z*); VI4Hy-4Me (994 *m*/*z*)
AOP-9	II or IIHy-MeQ (330 *m*/*z*); IV5Hy-4Me (682 *m*/*z*); IVHy-Me (660 *m*/*z*); IVHy-4Me, IVHyQ (672 *m*/*z*); VII3Hy-2Me (1170 *m*/*z*); IV2Hy-3Me (648 *m*/*z*); III2Hy (526 *m*/*z*); IV2Hy or IV3Hy-MeQ (690 *m*/*z*); III or IIIHy-MeQ (494 *m*/*z*); IV4Hy-3Me (680 *m*/*z*); IV or IVHy-MeQ (658 *m*/*z*); VHy (838 *m*/*z*)
AOP-10	II or IIHy-MeQ (330 *m*/*z*); IV5Hy-4Me (682 *m*/*z*); IVHyQ (672 *m*/*z*); IVHy-4Me (618 *m*/*z*); V-2Me (794 *m*/*z*); IV2Hy-2Me (662 *m*/*z*); VHy (838 *m*/*z*); IV2Hy or IV3Hy-MeQ (690 *m*/*z*); III or IIIHy-MeQ (494 *m*/*z*); IV4Hy-3Me (680 *m*/*z*); III-Me or IIIHy-2MeQ (480 *m*/*z*); IV-Me or IVHy-2MeQ (644 *m*/*z*); IHy-Me (168 *m*/*z*); IV4Hy-Me (694 *m*/*z*)

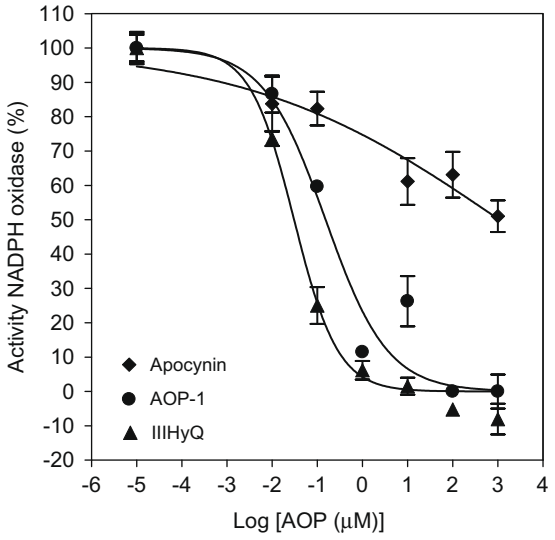

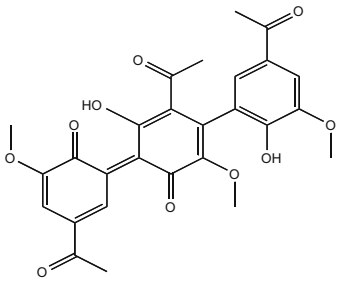

Trimer Quinone Hydroxylated IIIHyQ
Chemical Formula: $C_{27}H_{24}O_{10}$
Exact Mass: 508.1369

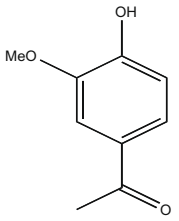

Apocynin

Chemical Formula: $C_9H_{10}O_3$
Exact Mass: 166.0630
Molecular Weight: 166.1739

Figure 1. Effect of apocynin, IIIHyQ, and AOP-1 on NADPH oxidase activity. Experiments were performed by reduction of cytochrome *c* using EC in a 96-well plate with AOP concentrations of 0–1 mM.

from the cytosol to bind to membrane-associated $p22^{phox}$ is a key event in the mechanism of NADPH oxidase activation and is presumably driven by the interaction of an SH3 domain on the $p47^{phox}$ with a proline-rich region on the $p22^{phox}$.[17,18] To ascertain whether the mechanism of AOP inhibition of NADPH oxidase is due to disruption of the interaction of $p47^{phox}$ with $p22^{phox}$, we performed a well-plate ELISA assay. Isolated IIIHyQ and the AOP-1 mixture were potent inhibitors of this interaction (Fig. 3; Table 2) with IC_{50} values of 1.60 μM and 0.55 μM, respectively. Apocynin had no effect on protein–peptide interaction.

Table 2
Dose–response IC_{50} values of AOP fractions following peroxidase-catalyzed oxidation of apocynin and silica gel chromatography

Fraction	Log(IC_{50}) (IC_{50} in parentheses, μM) Cell-based assay	Log(IC_{50}) (IC_{50} in parentheses, μM) ELISA assay
Apocynin	3.04 ± 0.49 (1090)	4.78 ± 6.65 (61,000)
IIIHyQ	−1.51 ± 0.05 (0.03)	0.20 ± 0.15 (1.60)
AOP-2	−1.40 ± 0.05 (0.04)	−0.27 ± 0.15 (0.55)
AOP-3	−0.61 ± 0.08 (0.25)	1.70 ± 0.15 (50.0)
AOP-4	−0.67 ± 0.10 (0.22)	0.47 ± 0.18 (2.96)
AOP-5	0.34 ± 0.11 (2.20)	0.44 ± 0.90 (7.96)
AOP-6	−0.09 ± 0.09 (0.82)	2.01 ± 0.16 (103)
AOP-7	0.001 ± 0.06 (1.00)	2.66 ± 456 (453)
AOP-8	0.03 ± 0.22 (1.08)	2.38 ± 0.08 (239)
AOP-9	−0.04 ± 0.13 (0.92)	1.54 ± 0.08 (34.8)
AOP-10	−0.11 ± 0.12 (0.78)	2.03 ± 0.08 (107)

We then evaluated the remaining AOP fractions for their ability to disrupt the interaction of $p47^{phox}$ with $p22^{phox}$ (Table 2). ELISA results followed a similar pattern to that observed in the cell based studies, with low activity in fractions consisting of higher oligomeric species. A plot of the log(IC_{50}) values from the cell-based assay and from ELISA (Fig. 4) shows good linear correlation (R^2 = 0.87), suggesting that VEC NADPH oxidase inhibition is likely explained by the ability of the AOP to disrupt the interaction of $p47^{phox}$ with $p22^{phox}$.

2.4. Proposed mechanism of AOP-mediated inhibition of NADPH oxidase

Apocynin was a poor inhibitor of NADPH oxidase in VEC-based assays, suggesting that previous results describing the effectiveness of apocynin as an NADPH oxidase inhibitor were a consequence of its conversion into active metabolites, likely catalyzed by peroxidases. In the present study, we produced the oligomers in vitro, which allowed the structural characterization of AOP. As a result, a trimer hydroxylated quinone (IIIHyQ) was identified as a strong inhibitor from AOP-1 and its structure was characterized by high resolution mass spectrometry (HRMS) and nuclear magnetic resonance (^{1}H NMR and ^{13}C NMR); detailed information on

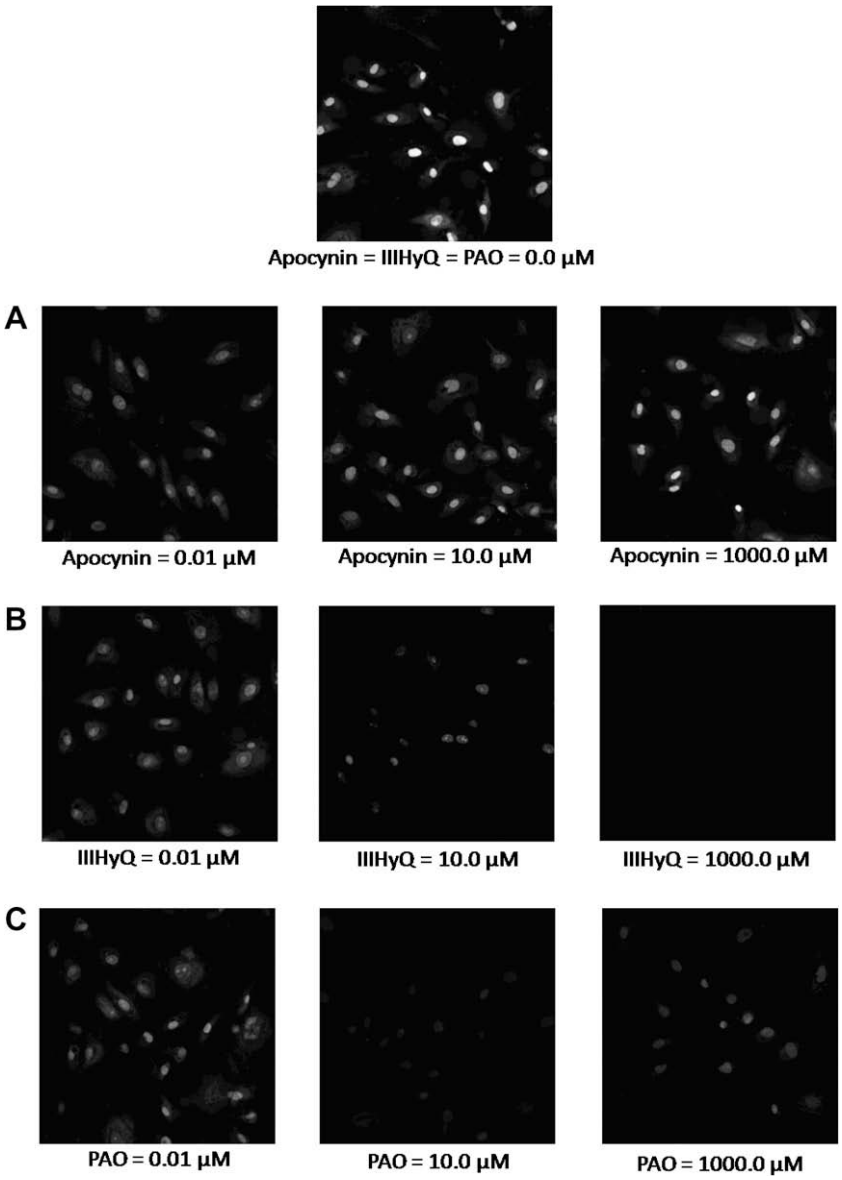

Figure 2. Intracellular detection of $\cdot O_2^-$ by DHE staining in EC. Cells were incubated with (A) Apocynin (B) IIIHyQ and (C) PAO. Dose range: 0–1 mM. Images were taken by confocal microscopy.

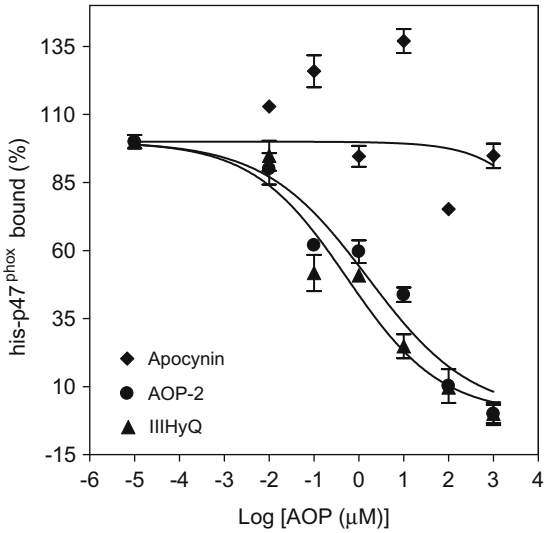

Figure 3. Effect of isolated IIIHyQ, AOP-2 and apocynin, on biotin-p22^{phox}–his-p47^{phox} interaction by ELISA. Biotin- p22^{phox} = 2.0 μM, his- p47^{phox} = 0.3 μM.

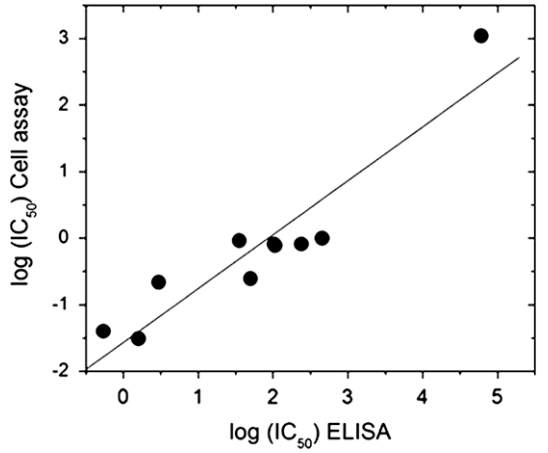

Figure 4. Correlation of experimental log(IC_{50}) values of cell-based assay and ELISA.

HRMS and NMR is provided in the Supplementary data. However, not all the oligomers were strong inhibitors. Dimeric and trimeric AOP were more effective inhibitors of VEC NADPH oxidase than higher order oligomers identified in fractions AOP-6 to AOP-10. A possible explanation is that large oligomers are poorly soluble in aqueous media and are, therefore less capable of interacting with key subunits of VEC NADPH to inhibit assembly.

One possible mechanism of inhibition is the ability of reactive metabolites (e.g., quinones such as IIIHyQ) to form Michael adducts with the cysteine residues of p47^{phox}.[40,41] This would be consistent with the known neutrophils NADPH oxidase inhibitor, phenylarsine oxide, which binds covalently with thiol groups in the enzyme, thereby preventing assembly of protein subunits.[42] Human p47^{phox} contains four cysteine residues at positions 98, 111, 196 and 378. Indeed, Cys-196 is located in one of the two SH3 domains of p47^{phox} (SH3-N, amino acids 156–215). As indicated above, the interaction of the p47^{phox} (in complex with the other cytosolic NADPH oxidase subunits) with the membrane-associated p22^{phox} occurs through this SH3 site on p47^{phox} with a PRR on p22^{phox}.[43] Modification of Cys-196 by quinone-containing may disrupt this critical interaction. However, one cannot rule out the modification of the other three cysteine residues, which may lead to additional structural changes of p47^{phox} that could disrupt binding of the p47^{phox} to the membrane or interaction of the p47^{phox} with PRR of the p67^{phox} subunit. This is a key part of the formation of the cytosolic complex[13,44,45] and is required for translocation of p67^{phox} to the membrane.[46,47]

To determine the importance of Cys on the interaction between p22^{phox} and p47^{phox} we examined the interaction of immobilized biotin-p22 (2 μM) with his-p47^{phox} (0–1.0 μM) in the presence of iodoacetamide (IAA) (Fig. 5), which reacts with thiol groups on cysteine residues. The presence of 1 μM IAA results in a >50% drop in the amount of bound p47 to the immobilized biotin-p22^{phox}; hence, thiol reactivity of quinone-based AOPs may be a critical mechanism of inhibition of VEC NADPH oxidase assembly.

In summary, we have demonstrated that peroxidase-generated apocynin metabolites serve as strong inhibitors of VEC NADPH oxidase. The IIIHyQ was a particularly strong (nanomolar) inhibitor of the enzyme as determined through EC-based assays. This compound was also effective at disrupting the p47^{phox}–p22^{phox} interaction in vitro. This suggests that the mechanism of apocynin inhibition of NADPH oxidase is a result of peroxidase metabolism to yield reactive quinones that bind to Cys residues in p47^{phox} and disrupt translocation to the membrane through SH3-PRR association with the p22^{phox}. Since peroxidases are common enzymes in the vasculature (e.g., myeloperoxidases) one may anticipate that similar metabolites are generated in vivo. Further work is needed to determine whether these metabolites provide a means to the generation of potential therapeutic molecules.

3. Experimental

Apocynin, SBP, solvents, H_2O_2, LDL, superoxide dismutase (SOD), low density lipoprotein (LDL), cytochrome *c*, Tween 20, 3,3′,5,5′-tetramethyl-benzidine (TMB), sodium caseinate, fetal bovine serum, heparin, and endothelial growth supplement were purchased from Sigma–Aldrich. Endothelial cells and medium were purchased from ATCC. *Escherichia coli* BL21 (DE3), IPTG and Ni-affinity column (Probond system) were purchased from Invitrogen. Antibodies were purchased from Upstate. High-affinity streptavidin-coated-96 well plates were purchased from Pierce. LC–MS analyses were performed in a Shimadzu LCMS-2010A. Samples for LC–MS were separated in an Agilent Zorbax 300SB-C_{18} column (5 μm, 2.1 × 150 mm). Silica gel 230–400 mesh was purchased from Natland International Corporation. Thin layer chromatography (TLC) plates were purchased from Merck. Microplate reader

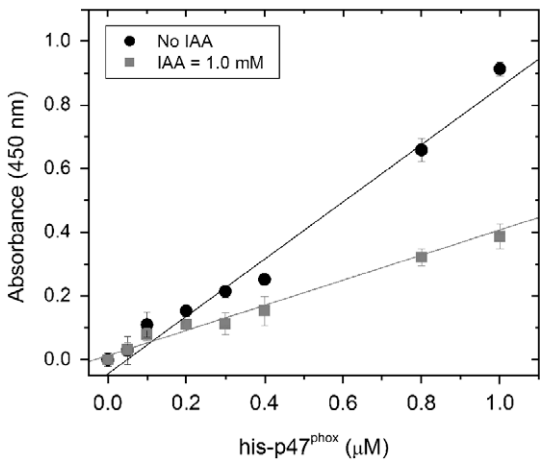

Figure 5. Interaction between biotin-p22^{phox} (2.0 μM) and his-p47^{phox} (0–1.0 μM) in the absence and presence of IAA (1.0 mM).

analyses were performed in a Perkin-Elmer, HTS 7000, Bio Assay Reader.

3.1. Enzymatic production of apocynin oxidation products (AOP)

AOP were synthesized by soybean peroxidase (SBP)-catalyzed oxidation of apocynin, as described by Antoniotti et al.[37] Briefly, apocynin (6 mmol) was dissolved in 5 mL of dimethylformamide (DMF) and transferred to 490 mL phosphate buffer (50 mM, pH 7). SBP (5 mL of a 1 mg/mL solution) was added and the reaction was initiated by using a syringe pump to introduce H_2O_2 (30% w/v) at 0.1 mL/min for 12 min to afford 12 mmol H_2O_2. Finally, the reaction was stopped after 2 h. Soluble and precipitated phases were separated by centrifugation and ethyl acetate was added to supernatant to extract organic compounds (AOP-1). Both precipitated and extracted supernatant fractions were dried and stored at −20 °C under argon.

3.2. Fractionation of non-soluble phase

The precipitated fraction (60 mg) was dissolved in the minimum amount of chloroform and loaded onto a silica gel column (flash chromatography, 4 g silica gel 230–400 mesh, Natland International Corporation) and eluted with a gradient of petroleum ether/ethyl acetate 2:1 to 0:1. Nine fractions (AOP-2 to AOP-10) were collected and analyzed by LC–MS (Shimadzu LCMS-2010A) using an Agilent Zorbax 300SB-C_{18} column, 5 μm, 2.1 × 150 mm with isocratic elution (MeCN/H_2O, 3:7; 0.2 mL/min).

3.3. Purification of the trimer hydroxylated quinone (IIIHyQ)

AOP-1 (290 mg) was dissolved in chloroform and loaded on a silica gel column (15 g) and eluted with a gradient of petroleum ether/ethyl acetate (2:1 to 0:1). Unmodified apocynin was recovered in the early fractions (210 mg, R_f 0.62 with petroleum ether/ethyl acetate, 1:1) and further elution with pure ethyl acetate furnished the IIIHyQ as a white powder (14 mg, R_f 0.34 with petroleum ether/ethyl acetate, 1:1). HRMS *m/z*, calculated for $C_{27}H_{25}O_{10}$ $[M+H]^+$ 509.1442, found 509.1442. Calculated for $C_{27}H_{24}O_{10}Na$ $[M+Na]^+$ 531.1258, found 531.1261. Calculated for $C_{27}H_{24}O_{10}K$ $[M+K]^+$ 547.1001, found 547.0997. ^1H NMR (500 MHZ, $CDCl_3$) 7.65 (1H, d, J = 1.5 Hz), 7.57 (1H, d, J = 1.8 Hz), 7.40 (1H, d, J = 1.5 Hz), 7.20 (1H, d, J = 1.5 Hz), 6.07 (1H, s), 4.05 (1H, s), 3.99 (3H, s), 3.98 (3H, s), 3.69 (3H, s), 2.57 (3H, s), 2.44 (3H, s), 2.18 (3H, s). ^{13}C NMR (125 MHZ, $CDCl_3$) 201.22, 196.02, 195.63, 195.46, 153.08, 148.88, 145.82, 144.94, 133.14, 132.85, 123.70, 121.53, 120.41, 119.30, 113.34, 111.62, 98.31, 90.18, 63.13, 62.59, 62.16, 56.40, 56.23, 53.21, 26.48, 26.29, 23.65. ^1H NMR and ^{13}C-NMR spectra were recorded at room temperature, in $CDCl_3$ (Varian 500 MHz or Bruker 600 MHz and 800 MHz). Chemical shifts (δ) are indicated in ppm and coupling constants (J) in Hz. Flash chromatography was performed using silica gel 230–400 mesh (Natland International Corporation). Thin layer chromatography (TLC) was carried out using Merck plates of Silica Gel 60 with fluorescent indicator and revealed with UV light (254 nm) and 5% H_2SO_4 in EtOH.

3.4. Endothelial cell culture

Human umbilical vascular endothelial cells (HUVEC; ATCC) were cultured in F-12 K medium supplemented with 10% (v/v) fetal bovine serum, heparin (0.1 mg/mL), and endothelial growth supplement (0.04 mg/mL). The medium was replenished every two days until confluence was achieved. The cells were propagated by detaching them with 0.25% (w/v) trypsin—0.53 mM EDTA solution, adding supplemented F-12 K medium and centrifuging, and then the cells were sub-cultured in new culture vessels until the desired number of cells was obtained.

3.5. NADPH oxidase activity—Cytochrome *c* reduction

The inhibitory effect of AOP on NADPH oxidase was assessed by the inhibition of $\cdot O_2^-$ generated by VEC and measured by reduction of cytochrome *c*.[16] Cells were resuspended in DMEM without phenol red and incubated in 96-well flat bottom culture plates (10^5 cells/mL) for 10 min at 37 °C in a humidified CO_2 incubator. Low density lipoprotein (100 μg/mL) was used to induce activation of NADPH oxidase. AOP were incubated at concentrations ranging from 0 to 1000 μM in the presence of 100 μM NADPH, with or without superoxide dismutase (SOD, 200 μg/mL), and in the presence of cytochrome *c* (250 μM) for 30 min at room temperature. Cytochrome *c* reduction was measured by reading absorbance at 550 nm in a microplate reader. Inhibition of NADPH oxidase was calculated from the difference between the absorbance of sample with or without SOD and the extinction coefficient for the change of oxidized cytochrome *c* to reduced cytochrome *c* (18.7 cm^{-1} mM^{-1}); experiments were performed in triplicate.

3.6. Intracellular superoxide production—DHE staining

Endothelial cells were incubated in black, clear-bottom 96-well cell binding surface plates and incubated with apocynin, IIIHyQ, or PAO at concentration ranging from 0 to 1 mM for 2 h in DMEM in the absence of phenol red. DMEM was removed and the cells were washed twice with PBS and then resuspended in fresh DMEM. NADPH oxidase was activated with phorbol myristate acetate (PMA, 1 μM) for 30 min and the cells were then incubated with DHE (3 μM) for 30 min and then NADPH (100 μM) to generate $\cdot O_2^-$; the experiment was performed in the dark. Cell images were captured after 30 min with a Zeiss LSM 510 laser scanning confocal microscope at excitation and emission wavelengths of 520 and 610 nm, respectively.

3.7. Production and purification of his-p47^{phox} and biotin-p22

A proline-rich p22^{phox} peptide N′-151PPSNPPPRPPAEARK165-C′, which was biotinalyted at the N-terminus and amidated at the C-terminus was obtained from Genemed Synthesis Inc. (South San Francisco, CA). The biotin group was attached through a 4-residue spacer consisting of SGSG. The purity of the peptide was 99.99%. Endothelial cell derived p47^{phox} DNA (6 His-tagged) was obtained from SUNY Albany and Stratton VA Medical Center and confirmed by DNA sequence analysis (U. of Maine). His-p47^{phox} protein was expressed in BL21 (DE3) cells for 9 h using 0.5 mM isopropyl-β-D-thiogalactopyranoside (IPTG) at 35 °C. The protein was purified using a Ni-affinity column (ProBond System) and confirmed by western blot analysis with anti p47^{phox} antibody and the purity (80%) was calculated with the Image J software (NIH, USA, public domain) based on the intensity of each protein band on the electrophoresis gel.

3.8. Biotin-p22. and his-p47^{phox} interaction

Interaction of p47^{phox} with the p22^{phox} peptide was studied using ELISA, which was modified from the technique reported by Dahan et al.[48] Experiments were performed in high-affinity streptavidin-coated-96 well plates. To block non-specific binding sites, each well was re-blocked with 300 μL of PBS supplemented with 0.1% (v/v) Tween 20 and 1% sodium caseinate. To each well, 100 μL of 2 μM biotin-p22^{phox} peptide solution were added and incubated at room temperature for 1 h. After washing each well

four-times with 300 μL PBS-Tween solution, 100 μL of 0.30 μM his-p47^{phox} (in PBS-Tween solution containing 1% sodium caseinate) and AOP (0–1000 μM) were added to each well and incubated at room temperature for 1 h. Unbound components were removed by washing four times with 300 μL/well PBS-Tween solution. The amounts of bound his-p47^{phox} were quantified by adding 100 μL/well of polyclonal goat anti-p47^{phox} (diluted 1:2000 in PBS-Tween solution containing 1% sodium caseinate) and incubating at room temperature for 1 h. Each well was washed four times with 300 μL PBS-Tween solution and incubated with 100 μL/well of HRP-conjugated rabbit anti-goat IgG secondary antibody (diluted 1:10000 in PBS-Tween solution containing 1% sodium caseinate) at room temperature for 1 h. The plate was finally washed four times with 300 μL/well of PBS-Tween solution and two additional washes with 300 μL/well of PBS. Detection of peroxidase activity was performed with a ready-to-use TMB liquid substrate by adding 200 μL/well and incubating at room temperature for 30 min. The reaction was terminated by adding 100 μL/well of 0.5 M H_2SO_4 solution and the absorbance was read at 450 nm in the microplate reader. All experiments were performed in triplicate and results were quantified from a standard curve of the interaction between biotin-p22^{phox} (2 μM) and his-p47^{phox} (0–0.40 μM).

Acknowledgments

We are grateful to NIH (AT002115) for the financial support of this project and to Dr. Christopher Bjornsson, Director of Microscopy and Imaging Core Facility (Center for Biotechnology and Interdisciplinary Studies, Rensselaer Polytechnic Institute), for his help with the confocal fluorescent microscopy analysis.

Supplementary data

Supplementary data associated with this article can be found, in the online version, at doi:10.1016/j.bmc.2009.05.061.

References and notes

1. Li, J.; Mullen, A.; Shah, A. J. *Mol. Cell Cardiol.* **2001**, *33*, 1119.
2. Touyz, R. M. *Hypertension* **2004**, *44*, 248.
3. Li, Q.; Subbulakshmi, V.; Fields, A. P.; Murray, N. R.; Cathcart, M. K. *J. Biol. Chem.* **1999**, *274*, 3764.
4. Walch, L.; Massade, L.; Dufilho, M.; Brunet, A.; Rendu, F. *Atherosclerosis* **2006**, *187*, 285.
5. Holland, J. A.; Ziegler, L. M.; Meyer, J. W. *J. Cell. Physiol.* **1996**, *166*, 144.
6. Lassegue, B.; Clempus, R. E. *Am. J. Physiol. Regul. Integr. Comp. Physiol.* **2003**, *285*, 277.
7. Babior, B. M. *Blood* **1999**, *93*, 1464.
8. Finkel, T. *Curr. Opin. Cell Biol.* **2003**, *15*, 247.
9. Meng, T. C.; Fukada, T.; Tonks, N. K. *Mol. Cell.* **2002**, *9*, 387.
10. Taniyama, Y.; Griendling, K. K. *Hypertension* **2003**, *42*, 1075.
11. Meyer, J. W.; Schmitt, M. E. *FEBS Lett.* **2000**, *472*, 1.
12. Seguchi, H.; Kobayashi, T. *J. Electron Microsc.* **2002**, *51*, 87.
13. Groemping, Y.; Rittinger, K. *Biochem. J.* **2005**, *386*, 401.
14. Gorlach, A.; Brandes, R. P.; Nguyen, K.; Amidi, M.; Dehghani, F.; Busse, R. *Circ. Res.* **2000**, *87*, 26.
15. Li, J.; Shah, A. M. *Cardiovasc. Res.* **2001**, *52*, 477.
16. Li, J. M.; Shah, A. M. *J. Biol. Chem.* **2002**, *277*, 19952.
17. Hiroaki, H.; Ago, T.; Ito, T.; Sumimoto, H.; Kohda, D. *Nat. Struct. Biol.* **2001**, *8*, 526.
18. Sumimoto, H.; Kage, Y.; Nunoi, H.; Sasaki, H.; Nose, T.; Fukumari, Y.; Ohno, M.; Minakami, S.; Takeshige, K. *Proc. Natl. Acad. Sci.* **1994**, *91*, 5345.
19. Martyn, K. D.; Frederick, L. M.; von Loehneysen, K.; Dinauer, M. C.; Knaus, U. G. *Cell. Signal.* **2006**, *18*, 69.
20. Kuroda, J.; Nakagawa, K.; Yamasaki, T.; Nakamura, K.; Takeya, R.; Kuribayashi, F.; Imajoh-Ohmi, S.; Igarashi, K.; Shibata, Y.; Sueishi, K.; Sumimoto, H. *Genes Cells* **2005**, *10*, 1139.
21. Li, J.; Fan, L. M.; George, V. T.; Brooks, G. *Free Radical Biol.* **2007**, *43*, 976.
22. Taura, M.; Miyano, K.; Miakaru, R.; Kamabura, S.; Takeya, R.; Sumimoto, H. *Biochem. J.* **2009** [Epub ahead of print].
23. Frey, R.S.; Ushio-Fukai, M.; Malik, A. *Antioxid. Redox Signal.* **2008** [Ahead of print].
24. Selemidis, S.; Dusting, G. J.; Peshavariya, H.; Kemp-Harper, B. K.; Drummond, G. R. *Cardiovasc. Res.* **2007**, *75*, 349.
25. Cayatte, A. J.; Rupin, A.; Oliver-Krasinski, J.; Maitland, K.; Sansilvestri-Morel, P.; Boussard, M.; Wierzbicki, M.; Verbeuren, T. J.; Cohen, R. A. *Arterioescler. Thromb. Vasc. Biol.* **2001**, *21*, 1577.
26. Shi, J.; Ross, C. R.; Leto, T. L.; Blecha, F. *Proc. Natl. Acad. Sci.* **1996**, *93*, 6014.
27. Kanegae, M. P. P.; da Fonseca, L. M.; Brunetti, I. L.; de Oliveira Silva, S.; Ximenes, V. F. *Biochem. Pharmacol.* **2007**, *74*, 457.
28. Yu, J.; Weiwer, M.; Linhardt, R.; Dordick, J. S. *Curr. Vasc. Pharmacol.* **2008**, *6*, 1.
29. Johnson, D. K.; Schillinger, K. J.; Kwait, D. M.; Hughes, C. V.; McNamara, E. J.; Ishmael, F.; O'Donnell, R. W.; Chang, M.; Hogg, M. G.; Dordick, J. S.; Santhanam, L.; Ziegler, L. M.; Holland, J. A. *Endothelium* **2002**, *9*, 191.
30. Heumüller, S.; Wind, S.; Barbosa-Sicard, E.; Schmidt, H. H. H. W.; Busse, R.; Schröeder, K.; Brandes, R. P. *Hypertension* **2008**, *51*, 211.
31. Vejraska, M.; Micek, R.; Stipek, S. *Biochim. Biophys. Acta* **2005**, *1722*, 143.
32. Dodd-O, J. M.; Pearse, D. B. *Am. J. Physiol. Heart Circ. Physiol.* **2000**, *279*, 303.
33. Muijers, R. B. R.; van den Worm, E.; Folkerts, G.; Beukelman, C. J.; Koster, A. S.; Postma, D. S.; Nijkamp, F. P. *Brit. J. Pharmacol.* **2000**, *130*, 932.
34. Chan, E. C.; Datla, S. R.; Dilley, R.; Hickey, H.; Drummond, G. R.; Dusting, G. J. *Cardiovasc. Res.* **2007**, *75*, 710.
35. Ximenes, V. F.; Kanegae, M. P. P.; Rissato, S. R.; Galhiane, M. S. *Arch. Biochem. Biophys.* **2007**, *457*, 134.
36. Stolk, J.; Hiltermann, T. J.; Dijkman, J. H.; Verhoeven, A. J. *Am. J. Respir. Cell Mol. Biol.* **1994**, *11*, 95.
37. Antoniotti, S.; Santhanam, L.; Ahuja, D.; Hogg, M.; Dordick, J. S. *Org. Lett.* **2004**, *6*, 1975.
38. Bendall, J. K.; Rinze, R.; Adlam, D.; Tatham, A. L.; de Bono, J.; Channon, K. M. *Circ. Res.* **2007**, *100*, 1016.
39. Doussiere, J.; Poinas, A.; Blais, C.; Vignais, P. *Eur. J. Biochem.* **1998**, *251*, 649.
40. 't Hart, B.A.; Simons, J.M.; Rijkers, G.T.; Hoogvliet, J.C.; Van Dijt, H.; Labadie, R.P. *Free Radical Biol. Med*. **1990**, *8*, 241.
41. Simons, J. M.; t' Hart, B. A.; Vai Ching, T.; van Dijk, H.; Labadie, R. P. *Free Radical Biol. Med.* **1990**, *8*, 251.
42. Le Cabec, V.; Maridonneau-Parini, I. *J. Biol. Chem.* **1995**, *270*, 2067.
43. Leto, T. L.; Adams, A. G.; De Mendez, I. *Proc. Natl. Acad. Sci.* **1994**, *91*, 10650.
44. Takeya, R.; Ueno, N.; Kami, K.; Taura, M.; Kohjima, M.; Izaki, T.; Nunoi, H.; Sumimoto, H. *J. Biol. Chem.* **2003**, *278*, 25234.
45. Lapouge, K.; Smith, S. J. M.; Groemping, Y.; Rittinger, K. *J. Biol. Chem.* **2002**, *277*, 10121.
46. Morozov, I.; Lotan, O.; Joseph, G.; Gorzalczany, Y.; Pick, E. *J. Biol. Chem.* **1998**, *273*, 15435.
47. Park, J. *Biochem. Biophys. Res. Commun.* **1996**, *220*, 31.
48. Dahan, I.; Issaeva, I.; Gorzalczany, Y.; Sigal, N.; Hirshberg, M. *J. Biol. Chem.* **2002**, *227*, 8421.